Arab Journal of Nuclear Science and Applications, 48(4), (219-236) 2015

Treatment of Total Reaction Cross Section for Proton and Antiproton Scattering from ^{3}He

I.M.A. Tag El-Din[1], S.S.A. Hassan[2], M.S.M. Nour El-Din[3] and A.H. Almekawy[4]

[1]*Experimental Nuclear Physics Dept., Nuclear Research Center, Atomic Energy Authority, Cairo , Egypt.*

[2] *Mathematics and Theor. Phys. Dept., Nuclear Research Center, Atomic Energy Authority, Cairo, Egypt.*

[3]*Physics Dept., Benha University, Benha, Egypt.*

[4]*Cycletron Project Nuclear Research Center, Atomic Energy Authority, Cairo, Egypt.*

Revived: 17/2/2015 **Accepted: 17/3/2015**

ABSTRACT

Within the framework of optical limit approximation (OLA) of Glauber multiple scattering model (GMSM), the total reaction cross section σ_R for proton and antiproton scattering from the target nucleus ^{3}He at incident energies, $18 < E_p \leq 1000$ MeV and $19 < E_{\bar{p}} < 1100$ MeV, are calculated. A model wave function with the effect of three-body force, harmonic oscillator and a Gaussian forms are used to describe the ground state density distribution of ^{3}He. The parameters of hadron-nucleon elastic scattering amplitude are taken to be both free and nuclear in-medium parameters. Introducing the phase variation parameter in conjunction with free, in-medium hadron –nucleon parameter, and with higher order momentum transfer components led to a satisfactory agreement with the available experimental data in case of p-^{3}He for$18 < E_p < 50$ MeV. In addition, it is found that the effects of both Pauli blocking and the geometrical law with effective proton-nucleon total cross-section play a significant role in describing σ_R at this range of proton energy. On the other hand, a more accurate result for σ_R in case of $\bar{p} - {}^3He$ at the only existing experimental data $E_{\bar{p}} = 19.6\ MeV$ is obtained by invoking the phase variation parameter with free parameters of $\bar{p} - nucleon$ elastic scattering amplitude.

Key words: Hadron scattering / Optical limit approximation / Nuclear In-Medium Effects.

I.INTRODUCTION

In recent years, the study of proton (p) and antiproton ($\bar{p}$) – nucleus total nuclear reaction cross section, σ_R [(1-7)] have attracted great attention**.**

Due to the increasing demand of well measured cross sections, especially for scattering of hadrons from light nuclei, where no much experimental data are available, scientists often need to rely on theoretical model calculations. The Glauber multiple scattering model (GMSM) [(8)] has been quite successful in describing the measured σ_R in intermediate and high energy regions. This model attributed all reactions for collisions between individual nucleons in the target and projectile. The model assumed that the projectile have a straight (Eikonal) trajectory during the scattering processes. For hadron-nucleus scattering, the hadron- nucleon elastic scattering amplitude and the nucleon density distribution of the target nucleus are two main ingredients of GMSM. The evaluation of higher order terms of GMSM is not only difficult for realistic description of nuclei, but also is beset with poor knowledge of higher order correlations in nuclei[(9)]. To overcome these difficulties many researchers

used what is called the optical limit approximation (OLA) taking into account nuclear in-medium correction to describe hadron-nucleus scattering[1,10,11]. The OLA, represents the first (leading) term of GMSM [8], where it describes the scattering of incident hadron with individual nucleons of the target nucleus (single scattering approximation).

One trust of relatively low and intermediate energy physics is the attempt to explain observed nuclear phenomena in terms of the nuclear sub-structure. In the strong interacting particles, the nucleus has been conventionally pictured as a system of nucleons interacting via meson exchange. In the simple form, the conventional model assumes that the properties of the nucleons inside the nucleus are unchanged from their free space values [12]. However, the higher values of initial data of k^+-nuclear scattering [13], and total cross sections [14], indicated that the properties of the nucleons in nuclear medium must be modified from free space values.

In GMSM model, the free-space hadron-nucleon total cross section $\sigma_{NN}(\text{free})$ which is obtained from the experimental measurements is used[8]. But the real nuclear in-medium hadron-nucleon total cross section $\sigma_{NN}(\text{in}-\text{med})$ is different from $\sigma_{NN}(\text{free})$ because of the effect of Pauli blocking and finite nuclear matter density.

It is well known that, the Pauli blocking suppresses the intermediate and final states of two-body scattering. Therefore, the in-medium nucleon-nucleon (NN) cross section $\sigma_{NN}(\text{in}-\text{med})$ is density dependent and becomes smaller than that in free space[15,16]. As a result, $\sigma_{NN}(\text{in}-\text{med})$ provides an immediate connection with the nucleon mean free path λ; one of the most fundamental quantities characterizing the propagation of nucleons through nuclear matter. In turn, λ enters in the determination of the nuclear transparency function where the latter is related to σ_R.

Many investigators[17-20] have studied the nuclear in-medium effects of the parameters of hadron-nucleon amplitude, especially, hadron-nucleon total cross- section , including their dependence on both the projectile incident energy and the density distribution of the target nucleus. Recently, Tag El-din et al[1] calculated the total reaction cross section for proton-^{4}He scattering using (OLA) within (GMSM) and Coulomb modified Glauber model (CMGM). A small contribution for the Coulomb effect within (CMGM) was found. They obtained a remarkable agreement at lower proton range of energy from 20 MeV to 50 MeV. This was done by introducing the effects of: phenomenological in-medium total nucleon-nucleon (NN) cross sections, NN phase variation and higher order momentum transfer component of NN elastic scattering amplitude, in addition to the effect of Pauli blocking. Those effects led to improve the results of OLA in describing hadron-nucleus scattering. Unfortunately, up to now, these in-medium effects and density distributions have not been well established for the calculations of $\sigma_{R..}$

The main objective of the present work is to treat the total nuclear reaction cross sections for proton and antiproton - ^{3}He using OLA of GMSM. Different nuclear in-medium effects are taken into consideration via (NN) scattering amplitude. In addition both three-body and repulsive NN short range forces are included in the model density of ^{3}He.

The paper is organized as follows: The mathematical formalism for σ_R within OLA is presented in section II. Section III is devoted to the numerical calculation of σ_R and the discussion in terms of different nuclear in-medium effects. Finally, a brief summery and concluding remarks are given in section IV.

II. Mathematical Formulation

The standard GMSM for the nuclear total reaction cross section is expressed as[8] ,

$$\sigma_R = 2\pi \int_0^\infty bdb\,[1-T(b)] \quad , \tag{1}$$

where T(b), the transparency function, is the probability that at an impact parameter b , the projectile passes through the target without interaction.
T(b) can be written as,

$$T(b) = \exp\{-2\,\mathrm{Im}\,\chi_N(b)\} \quad , \tag{2}$$

where $\chi_N(b)$ represents the nuclear phase shift function, which can be defined from OLA, as,

$$\chi_N^{OLA}(b) = iA \int \rho(\bar{r})\ \Gamma(\bar{b}-\bar{s})\, d\bar{r} \tag{3}$$

$\rho(\bar{r})$ and A refer to the ground state density distribution and the mass number of the target nucleus respectively, $\Gamma(\bar{b}-\bar{s})$ describes the nucleon-nucleon profile function, which is related to forward scattering free nucleon-nucleon (NN) amplitude $f_{NN}(q)$ by the relation[8] ,

$$\Gamma(\bar{b}-\bar{s}) = \frac{1}{2\pi ik}\int e^{i\bar{q}\bullet(\bar{b}-\bar{s})} f_{NN}(q)\, d^2q \tag{4}$$

Here, $\bar{s}$ is the projection of the target nucleon coordinate on the impact plane, and $\bar{q}$ being the momentum transfer of the incident particle. f_{NN} (q) in the presence of NN phase variation parameter and higher order momentum transfer components , can be expressed as[21],

$$f_{NN}(q) = \frac{k\sigma^t_{NN}}{4\pi}(i+\varepsilon_{NN})\, e^{-\frac{1}{2}(\beta_{NN}+i\gamma_{NN})q^2}[1+T(q)] \tag{5}$$

with,

$$T(q) = \sum_{n=1,2,\ldots} \lambda_n\, q^{2(n+1)} \tag{6}$$

σ^t_{NN} , ε_{NN} and β_{NN} are the hadron-nucleon total cross section, ratio of real-to-imaginary forward scattering amplitude (q = 0) and the slope parameter, respectively. K stands for the incident momentum of the hadron in the center of mass system. λ_n are free parameters. In the present work, n is taken to be equal to 1 and 2.It is well known that NN scattering measurements leave an overall phase of the amplitude undetermined. The phase factor $e^{i\gamma_{NN}q^2}$ in Eq.(5) takes care of this fact[22]. It is found that the parameters γ_{NN} and λ provide a remarkable improvement in the calculation of nucleus-nucleus[21] and proton-nucleus reaction cross sections[1] .

In this study, a model wave function describes the systematic S-state of the target nucleus, ^{3}He, can be written as [23, 24],

$$\psi(x,y,z) = N(1-2\gamma_{3BF}L)^{1/2}\,\alpha^3 x\,y\,z\,\exp[-\frac{\alpha^2}{2}(x^2+y^2+z^2)] \qquad (7)$$

where N is a normalization constant, α is the radius parameter, ($\gamma_{3BF} > 0$) represents the contribution weight of three-body force(3BF) in the model wave function and x, y, z stand for the intermediate distances. xyz is to simulate the effect of the short-range repulsion in two-body forces. The function L is expressed as,

$$L = \sum_i L_i \qquad , L_i = 3\cos^2\vartheta_i - 1 \qquad , i = x, y, z \qquad (8)$$

where $\cos\vartheta_z = \bar{x}\bullet\bar{y}/xy$ and $\sum_i$ implies the cyclic summation over x, y and z. The angular dependent term L represents the two-pion-exchange three-body force. Using suitable transformation, one can express the point proton density distribution of ^{3}He [23, 24] as,

$$\rho(r) = \frac{5\rho_\circ(r) - 6\gamma\,\rho_1(r)}{5 - 6\,\gamma_{3BF}} \qquad (9)$$

where

$$\rho_\circ(r) = \frac{7}{40}\left(\frac{3\alpha}{2\sqrt{\pi}}\right)^3 e^{-c^2/2}\left(1+\frac{2}{7}c^2+\frac{9}{35}c^4\right) \qquad (10)$$

$$\rho_1(r) = \frac{7}{4}\left(\frac{3\alpha}{2\sqrt{\pi}}\right)^3 e^{-c^2/2}\left(1-\frac{4}{7}c^2+\frac{3}{35}c^4\right) \qquad , c = 3\alpha r \qquad (11)$$

$\rho(r)$, $\rho_\circ(r)$ and $\rho_1(r)$ are normalized to unity. It is important to notice that, taking γ_{3BF} = 0 means that the contribution of 3BF is excluded, while the short-range effect still exist. The mean square radius of this density distribution [23] is given by,

$$< r^2 > = \frac{2}{3\alpha^2} \qquad (12)$$

which is independent on γ_{3BF}. The parameter α can be determined by taking into account $< r^2 > = r^2_{rms}(^3He) - r^2_{rms}(proton)$, where $r^2_{rms}(^3He)$ = 1.88 fm [25] and $r_{rms}(proton)$ =0.88 fm[26] . Therefore, the value of α becomes, 0.4915 fm. It was found that the value of the parameter γ_{3BF} which gives a best agreement in comparison with experimental data of p-^{3}He form factor is 0.02[23] , another values γ_{3BF} = 0 and 0.04 are tested[25].

For comparison, another two forms of charge density distributions where no short-range correlation and 3BF effects are included [25] ,

$$\rho_2(r) = \frac{z}{8\pi^{3/2}}\left[\frac{1}{a^3}e^{-r^2/4a^2} - \frac{h^2(6d^2-r^2)}{4d^7}e^{-r^2/4d^2}\right] \qquad (13)$$

The best fit values for the parameters of Eq. (13) are a = 0.675 ± 0.008 fm , h = 0.366 ± 0.025 fm and d = 0.836 ± 0.032 fm[25] . This distribution gives an excellent fit to the ^{3}He charge form factor up to q^2 = 8 fm^{-2} [25]. This form of density can be reduced to Gaussian form at h=0, then the parameter a is adjusted to reproduce the root- mean square radius of ^{3}He nucleus; $\langle r^2\rangle^{1/2}$, where $\langle r^2\rangle = 6a^2$ and $\langle r^2\rangle^{1/2} = 1.68\ \text{fm}$[23] , therefore a=0.68588fm.

There is a renewed interest in nucleon-nucleon (NN) scattering in nuclear medium, since in-medium NN cross –sections are important input parameters for various model calculations of nuclear dynamical processes [27].

The parameters of NN elastic scattering amplitude of Eq.(5) are considered as follows:

(1) The total cross-section (σ^t_{NN}) is taken as an average of both proton-proton (pp) and proton-neutron(pn) total cross-sections from the relation,

$$\sigma^t_{NN} = \frac{Z\sigma_{pp} + N\sigma_{pn}}{A} \qquad (14)$$

Z and N are the proton and neutron numbers, respectively. Three different parameterizations for σ_{pp} and σ_{pn} according to free nucleon-nucleon cross section (energy dependence) and in-medium nucleon-nucleon cross section (energy and density dependence) , according to:

(i) New fit [28] to the free nucleon-nucleon cross sections $\sigma^t_{NN}(\text{free})$ which are taken from the particle Data Group. This can be expressed as,

$$\left.\begin{aligned}\sigma_{pp}(E_p) &= 19.6 + 4253/E - 375/\sqrt{E} + 3.86\times10^{-2}E \ (\text{for } E_p < 280\ \text{MeV})\\ \sigma_{pn}(E_p) &= 89.4 - 2025/\sqrt{E} + 19108/E - 43535/E^2 \ (\text{for } E_p < 300\ \text{MeV})\end{aligned}\right\} \qquad (15)$$

(ii) In-medium total nucleon-nucleon cross section for proton energy from 10 to 1000 MeV [16] arising from the combination of free nucleon-nucleon total cross sections as parameterized in [20] with Dirac-Brueckner theory [18].

This parameterization can be written as,

$$\left.\begin{aligned}\sigma_{pp}(E_p,\rho) &= \left[13.73 - 15.04\,\eta^{-1} + 8.76\,\eta^{-2} + 68.67\,\eta^4\right]\times\frac{1+7.772E^{0.06}\rho^{1.48}}{1+18.01\rho^{1.46}}\\ \sigma_{pn}(E_p,\rho) &= \left[-70.67 - 18.18\,\eta^{-1} + 25.26\,\beta^{-2} + 113.85\,\eta^4\right]\times\frac{1+20.88E^{0.04}\rho^{2.02}}{1+35.85\rho^{1.9}}\end{aligned}\right\} \qquad (16)$$

where $\eta = \sqrt{1-1/\omega}$ and $\omega = E\,(\text{MeV})/931.5 + 1$. E is the incident proton energy in laboratory frame and ρ is the nuclear matter density in the unit of fm^{-3} . Eq.(16) is denoted by the phenomenological parameterization, so the resulting σ^t_{NN} is $\sigma^t_{NN}(\text{phenom})$ in units of mb and $\rho = \rho_\circ = 0.17\ \text{fm}^{-3}$, where $\rho_\circ$ is the saturation density of normal nuclear matter.

(iii) In-medium NN total cross sections [27], which are extracted from reaction matrices of the non-relativistic Brueckner approach. These non-relativistic cross sections are found to be reduced from free ones as observed in relativistic Brueckner calculations, where this reduction is ascribed to the flux renormalization represented by an effective mass. Within this approach, both in-medium σ_{pp} and σ_{pn} in units of mb can be formulated in the energy range $30 \leq E_p \leq 300$ MeV as

$$\left.\begin{aligned}\sigma_{pp}(E_p,\rho) &= a_1(1+a_2\sqrt{\rho}+a_3\rho)+\frac{a_4(1+a_5\rho)\sqrt{E_p/E_\circ}+a_6+a_7\sqrt{\rho}}{(E_p/E_\circ)+(a_8+a_9\sqrt{\rho}+a_{10}\rho)\sqrt{E_p/E_\circ}+a_{11}+a_{12}\sqrt{\rho}}\\ \sigma_{pn}(E_p,\rho) &= b_1(1+b_2\sqrt{\rho}+b_3\rho)+\frac{b_4(1+b_5\rho)\sqrt{E_p/E_\circ}+b_6+b_7\sqrt{\rho}}{(\sqrt{E_p/E_\circ})\;E_p/E_\circ+(b_8+b_9\sqrt{\rho}+b_{10}\rho)\sqrt{E_p/E_\circ}+b_{11}+b_{12}\sqrt{\rho}}\end{aligned}\right\} \quad (17)$$

where $E_\circ$ = 100 MeV is included for a convenient scale and $\rho = \rho_\circ = 0.17\,\mathrm{fm}^{-3}$. The numerical values of a_i and b_i in Eq.(17) are taken from Tables I and II with / without flux renormalization , respectively[27]. This is denoted by $\sigma^t_{NN}(\mathrm{in-med1})$ and $\sigma^t_{NN}(\mathrm{in-med2})$, respectively.

(iv) The experimental NN data from 30 to 1000 MeV as listed in [5].
Coming to the slope parameter β_{NN} , it is not a well determined quantity. Therefore, numerous of theoretical studies have been discussed the applicability of different values of β in proton-nucleus reaction cross section [5, 11] at relatively low and intermediate energies.

In this work, the slope parameter β_{NN} is determined from its relation to σ^t_{NN} and ε_{NN} according to the formula [5, 6, 29],

$$\sigma^{el}_{NN} = \frac{1+\varepsilon^2_{NN}}{16\pi\,\beta_{NN}}(\sigma^t_{NN})^2 \quad (18)$$

where, σ^{el}_{NN} represents the total elastic NN cross section. For E_p <300 MeV, only the elastic scattering is energetically possible as the pion production threshold is closed, so one can expect that $\sigma^{el}_{NN} = \sigma^t_{NN}$ [29].
This permits us to include the in-medium effect in the values of β_{NN}. At higher energies above 300 MeV, β_{NN} is chosen from the experimental data [5].

The ratio of real-to-imaginary forward elastic scattering amplitude for proton – proton (ε^{pp}_{NN}) and proton –neutron (ε^{pn}_{NN}) are parameterized from the phase shifts and Coulomb interference measurements as [11, 21],

$$\left.\begin{aligned}\varepsilon_{NN}^{pp} &= -0.386 + 1.224\, e^{-\frac{1}{2}\left(\frac{k-0.427}{0.178}\right)^2} + 1.01\, e^{-\frac{1}{2}\left(\frac{k-0.592}{0.638}\right)^2} \\ \varepsilon_{NN}^{pn} &= -0.666 + 1.437\, e^{-\frac{1}{2}\left(\frac{k-0.412}{0.196}\right)^2} + 0.617\, e^{-\frac{1}{2}\left(\frac{k-0.797}{0.291}\right)^2}\end{aligned}\right\} \quad (19)$$

k is the incident nucleon laboratory momentum in units of GeV/c. The values of k can be computed from the relation [1]

$$k = c\sqrt{E_p\,(E_p + 2m_p)} \quad (20)$$

The average value of ε_{NN} can be extracted from ε_{NN}^{pp} and ε_{NN}^{pn} obtained by,

$$\varepsilon_{NN} = \frac{z\,\sigma_{pp}\,\varepsilon_{NN}^{pp} + N\sigma_{pn}\,\varepsilon_{NN}^{pn}}{z\,\sigma_{pp} + N\sigma_{pn}} \quad (21)$$

Clearly, in-medium effect is also included in ε_{NN} via the values of σ_{pp} and σ_{pn}.

The parameters of antiproton-nucleon $(\bar{p}\,N)$ elastic scattering amplitude (Eq. 5) are considered from the fitting with experimental data in the energy range from 21 MeV to 1840 MeV [7] in the calculation of $\bar{p} - {}^{12}C$ total reaction cross-section,

$$\sigma_{\bar{p}N}^{t} = 81.3\ \text{fm}^2(\text{MeV})^{1/3} \bullet E_{\bar{p}}(\text{MeV})^{-1/3} \quad (22)$$

$$\beta_{\bar{p}N} = 0.4319(\text{fm}^2) + \frac{79.167(\text{MeV.fm}^2)}{E_{\bar{p}}(\text{MeV}) + 38.943(\text{MeV})} \quad (23)$$

$$\varepsilon_{\bar{p}N} = 0.141 - \frac{31.2(\text{MeV})}{E_{\bar{p}}(\text{MeV}) + 38.943(\text{MeV})} \quad (24)$$

These parameterization succeeded in describing σ_R for $\bar{p} - {}^{12}C$ in the above range of energy[7].

Throughout the present work both λ_n and γ_{NN} are considered as a free parameters.

III. RESULTS AND DISCUSSION

Firstly, p-^{3}He total Reaction cross section is calculated for the proton energy range from 40 to1000 MeV within OLA, using three different forms of ground state density distributions of ^{3}He as represented by Eqs.(9), (13) and (13) with h=0. The NN parameters are taken from the experimental free NN data [5] .Table (1) reveals the calculated values of σ_R. It is clear that the effects of three-body force with γ_{3BF} =0.02 and 0.04 is very small and can be neglected. The results of σ_R with harmonic oscillator density, Eq.(13) is higher than the corresponding values using the density distribution of Eq.(9), when γ_{3BF} = 0, by about 4 %. These differences may be attributed to the effect of short-range correlations in Eq.(9), which lead to some decrease in σ_R. At γ_{3BF} = 0, the results of σ_R arising from the Gaussian density (Eq.(13), h=0) is almost the same as extracted using the density

of Eq.(9). Moreover, an unsatisfactory agreement is found in comparison with the experimental data is obtained at E_p = 40MeV, where the calculation is overestimated the data by about 33% using Eq.(9) and by 37% using Eq.(13).

Since the experimental data for σ_R are available in the energy range of proton from 18.25 to 47.65 MeV[30], so, σ_R is calculated in this range of energy. Figs.(1) and (2) display our results by considering the model density of Eq.(9) with $\gamma_{3BF} = 0$ and density of Eq.(13), respectively. In addition, it is taken that $\gamma_{NN} = \lambda_n = 0$ and $\sigma^t_{NN}(\text{free})$ is evaluated from Eq.(15) . $\sigma^t_{NN}(\text{phenom})$ from Eq(16), both $\sigma^t_{NN}(\text{in}-\text{med1})$ and $\sigma^t_{NN}(\text{im}-\text{med2})$ from Eq.(17) are taken into account with $\rho = \rho_\circ = 0.17$ fm^{-3}. In general, no pronounced agreement is noticed by introducing $\sigma^t_{NN}(\text{free})$, where this is seen at 40 MeV in Table 1.

However, a better agreement is obtained for E_p> 25 MeV using both $\sigma^t_{NN}(\text{in}-\text{med1})$ and $\sigma^t_{NN}(\text{in}-\text{med2})$, but discrepancies are still exist over all this region using $\sigma^t_{NN}(\text{phenom})$.

Actually, in-medium reduction of σ^t_{NN} increases the transmission function T(b) , Eq.(1), which reduces the values of σ_R [31].

In an attempt to see if the agreement can be improved as previously discussed by Ibrahim et al[1] , we adopted the phase variation of NN elastic scattering amplitude via introducing the phase variation parameter, γ_{NN} (Eq.(5)). In addition, we consider only $\sigma^t_{NN}(\text{phenom})$ and $\gamma_{3BF} = \lambda_n = 0$.

Figs.(3) and (4) manifest a reliable agreement with the experimental data by invoking γ_{NN} using the density of Eq.(9) within two cases $\rho = \rho_\circ = 0$ fm^{-3} (Fig.(3)) and $\rho = \rho_\circ = 0.17$ fm^{-3} (Fig.(4)). It is apparent that γ_{NN} has always negative values and shows a systematic change with the incident proton energy.

Moreover, Figs.(5) and (6) reveal a satisfactory fitting with the experimental data using the density of Eq.(13) in two cases $\rho = \rho_\circ = 0$ fm^{-3} (Fig.(5)) and $\rho = \rho_\circ = 0.17$ fm^{-3} (Fig.(6)). The same systematic variation of γ_{NN} with incident proton energies is noticed. The values of γ_{NN} in the above four figures denote a clear dependence on both the density of target nucleus and energy of the incident proton. There is no unique value for γ_{NN} to estimate σ_R in the whole energy range.

The comparison between the predicted values of σ_R in Figs.(1) and (2) (dashed lines) and Figs.(3-6) (solid lines) with / without γ_{NN} shows that this phase pushes the OLA of GMSM closer to the experimental data. The physics of this phase may be well understood in terms of the partial wave analysis, where it is very clear how does the phase of free particle change due to the interaction after collision has taken place. Moreover, if we are using the parameters (σ^t_{NN} , ε_{NN} and β_{NN}) of free NN amplitude, then the value of the phase can be fixed from the analysis of nucleon-nucleus collision and in that case γ_{NN} could be taken as corresponding to the free NN amplitude. On the other hand, if the parameters (σ^t_{NN} , ε_{NN} and β_{NN}) take care of nuclear in-medium effects, then γ_{NN} obtained in this case may be considered as its in-medium values.

Introducing the NN elastic scattering amplitude with the second term, i.e. the higher order momentum transfer components with n =1 and 2 accompanied with γ_{NN} , a noticeable explanation of the experimental data is obtained using Eq.(9) as shown in Fig.(7) and Eq.(13) as presented in Fig.(8). Table (2) illustrates the values of λ_n at corresponding proton energies. It is obvious that, considering the higher order momentum transfer components affect the values of γ_{NN} , which become different from those for the case $\lambda_n = 0$. The real and imaginary values of λ_1 and λ_2 show a systematic decreasing with incident proton energy in the energy range under consideration. Also, a negative sign for imaginary part of λ_2 is obtained, as noticed in the work of [21].

The sign and the values of γ_{NN} are discussed for p-^{4}He total reaction cross-section in the proton energy range from 20 MeV to 1 GeV[1]. It is found that $\gamma_{NN} = -1.6\ \mathrm{fm}^2$ at ($\rho = \rho_\circ = 0$) and $\gamma_{NN} = -0.2\ \mathrm{fm}^2$ at ($\rho = \rho_\circ = 0.17\ \mathrm{fm}^{-3}$) give a best results for σ_R . These two values and the present values are different from those reported by many works[32-34]. On the other hand, Deeksha and Khan[21] obtained a good agreement for σ_R to α – nucleus scattering by invoking a set of γ_{NN} parameters at different energies. They concluded that another set of parameters for γ_{NN} (not shown in the paper) gave an agreement with the experimental data.

In this connection, it may be emphasized that because there is no way to connect γ_{NN} with the existing NN scattering observables, it is not possible to assess which one of the two sets of γ_{NN} values corresponds to the exact behavior of the NN amplitude in a given situation. They conclude that, considering the sole variation of NN phase could be different not only for different target nuclei, but also for different incident energies/nucleon.

At low incident energy, where mean-field effects prevail, NN collisions are strongly suppressed due to the fermionic nature of nucleons, known as Pauli blocking. The nucleon mean free path is large, typically larger than the nucleus size for incident energy, $E_{in/A} < 100\,\mathrm{MeV}$, and decreases towards a saturation value $\lambda_{nn} = 4-5\ \mathrm{fm}$ at high incident energy, for $E_{in/A} \geq 100\,\mathrm{MeV}$ [35]. Thus, the situation at high energy, where λ_{nn} is supposed to be almost constant, is quite clear. This is not the case in the Fermi energy domain , indeed, in-medium effects and especially quenching factors for NN total cross section are largely unknown in the range $E_{in/A} = 10-100\,\mathrm{MeV}$ and have to be constrained experimentally[36]. Therefore, the in-medium (effective) NN, the total cross section can be extracted due to Pauli blocking in this energy range from the relation [1,36,37],

$$\sigma_{eff}^{NN} = \sigma_{NN}^{t}(\mathrm{free})\left(1-\frac{7\alpha}{5}\frac{E_F}{E}\right) \qquad (25)$$

where $E = E_F + E_{inc}$, E_F =38.4 MeV, which corresponds to Fermi momentum $K_F = 1.38\ \mathrm{fm}^{-1}$ and E_{inc} is the incident proton energy.

Fig.(9) displays an acceptable agreement in comparison with the experimental data using σ_{eff}^{NN} , with both densities of Eqs.(9) and (13). The values of α are adjusted as shown in the figure, where it varies smoothly with energy and has values around unity, but not equal to one.

Moreover, it has been found that σ_R obeys the black sphere nucleus (BS) approximation [38] for proton energy, $E_p > 500\,MeV$. In this approximation σ_R is related to both the mass number A and the reduced cross section $\sigma_\circ$ by the relation [38],

$$\sigma_R(BS) = \sigma_\circ A^{\delta} \qquad (26)$$

The usual value of the power-law exponent δ, is considered to be 2/3[38] , while $\sigma_\circ$ is a varying parameter with incident proton energy. In the study of proton- nucleus total reaction cross section in the energy range of proton from 30 MeV to 2200 MeV using OLA, it is apparent that the results of σ_R at $E_p \geq 800$ MeV is obtained by adjusting the values of $\sigma_\circ$ as 52±0.3mb, 54 ±0.2 mb and 55±0.2 mb and δ =0.648 for proton scattering from $^6Li, ^9Be$ and ^8B, respectively.

In this work, Fig.(10) illustrates the application of Eq.(26) with δ = 2/3 and $\sigma_\circ$ is adjusted to be equal σ_{eff}^{NN} from Eq.(25). Indeed, a reasonable good fitting of the data is achieved. However, at E_p> 100 MeV, a plausible results within 10-15 % using $\sigma_\circ = \sigma_{NN}^{t}(free)$ are estimated.

Finally, it is found that our results are in good agreement in comparison with the work of Alvi [39], where σ_R is calculated from the analytical expression which has been derived from Coulomb modified Glauber (CMGM).In addition, a satisfactory agreement is obtained in comparison with the application of GMSM up to the second term using harmonic oscillator shell model density [40].

On the other hand, σ_R for $\bar{p} - {}^3He$ is calculated in the range of energy from 19.6 MeV to 1070 MeV using the above forms of density distributions for ^3He and $\bar{p}N$ parameters from Eqs.(22-24). Table (3) illustrates that there is no effect for the three body force on the values of σ_R. Fig.(11) show the results of σ_R with $\gamma_{3BF} = \lambda_n = 0$ in comparison with the only experimental data at 19.6 MeV, $\sigma_R = 392 \pm 23\,mb$ [41]. One can notice that our results are compatible with the work of Uzikov et al.[41] using Glauber- Sitenko approach[42] with $\bar{p}N$ amplitude (A) and (D), where all the results are within the experimental error at 19.6 MeV. Introducing γ_{NN} improve very well the agreement with the experimental data at 19.6 MeV (Table (4)), where it increases the value of σ_R with $\gamma_{NN} = -3\,fm^2$ for both the model and Gaussian densities, while it decreases the value of σ_R using the oscillator density. This behavior is in contrary with the case of p-^{3}He, where the negative values of γ_{NN} decrease the values of σ_R.

CONCLUSION

Although, the microscopic study of proton total reaction cross section on light nuclei seems not to have been addressed yet, σ_R for p-^{3}He is calculated using OLA considering in-medium NN parameters and three different densities for the target nucleus.

The comparison of the predicted values of σ_R with and without the phase of NN amplitude shows that the consideration of this phase brings the results of σ_R closer to the experimental data. The values of the phase variation parameter γ_{NN} show a consistent change with the incident proton energy for a given target nucleus, suggesting the phase could be different at different incident energies even if the interacting nucleons move in the same target nucleus. Also, the higher order components of the momentum transfer in conjunction with γ_{NN} gave a significant results for σ_R.

The effect of three body force (3BF) within the wave function of the target nucleus on σ_R seems to be small and can be neglected. Introducing this effect through hadron-nucleon profile function may change the situation. This point needs to be clarified in the future work.

Table (1): σ_R for p – ^{3}He, the experimental data are from[30].

E_p (MeV)	σ_R (mb)					
	Using eq. 9			Using eq. 13 with h=0	Using eq. 13	Exp. data
	γ_{3Bf} =0	γ_{3Bf} =0.02	γ_{3Bf} =0.04			
40	172.48	172.46	172.45	173.05	185.56	115 ± 5
60	133.56	133.57	133.58	133.29	141.17	
80	110.96	110.98	111.00	110.5	116.10	
100	96.50	96.52	96.54	95.98	100.39	
120	86.82	86.84	86.86	86.29	90.02	
140	80.07	80.09	80.10	79.54	82.86	
160	75.16	75.17	75.19	74.63	77.66	
180	71.66	71.67	71.68	71.13	73.99	
200	68.89	68.90	68.91	68.36	71.08	
240	65.28	65.28	65.29	64.75	67.29	
300	64.11	64.12	64.12	63.58	66.11	
425	65.16	65.16	65.16	64.62	67.23	
550	74.33	74.33	74.34	73.75	77.06	
650	82.95	82.96	82.96	82.36	86.33	
700	86.13	86.14	86.15	85.55	89.77	
800	88.44	88.46	88.46	87.87	92.23	
1000	89.26	89.28	89.29	88.69	93.03	

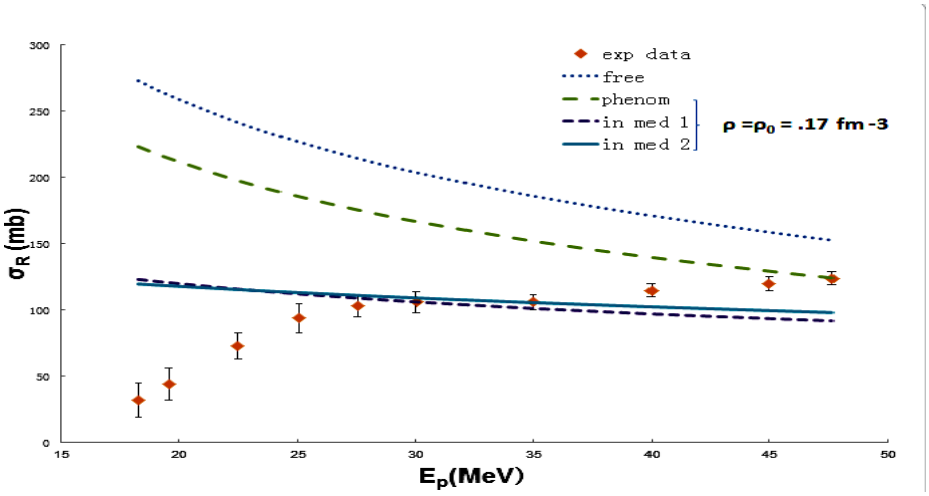

Fig. (1): Total reaction cross section for p-^{3}He using density distribution of Eq.(9), with different free and in -medium total cross sections, β is taken from Eq.(18),$\gamma_{NN} = \gamma_{3BF} = \lambda = 0$. The experimental data are those of Carlson [30].

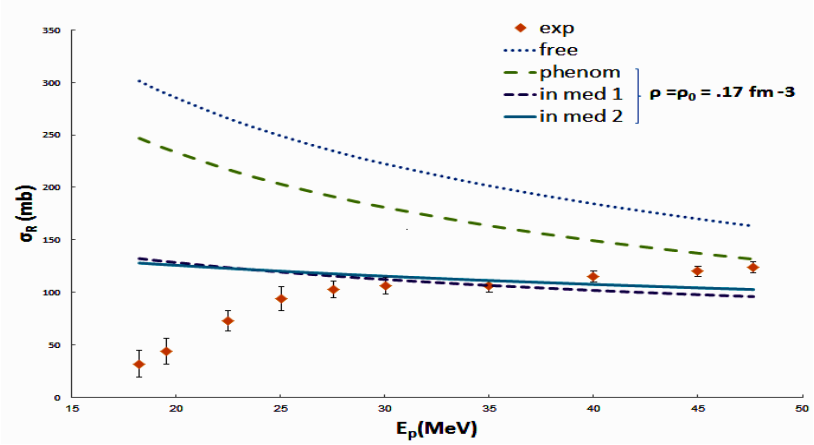

Fig. (2): As Fig.(1) but using the density distribution of Eq. (13) .

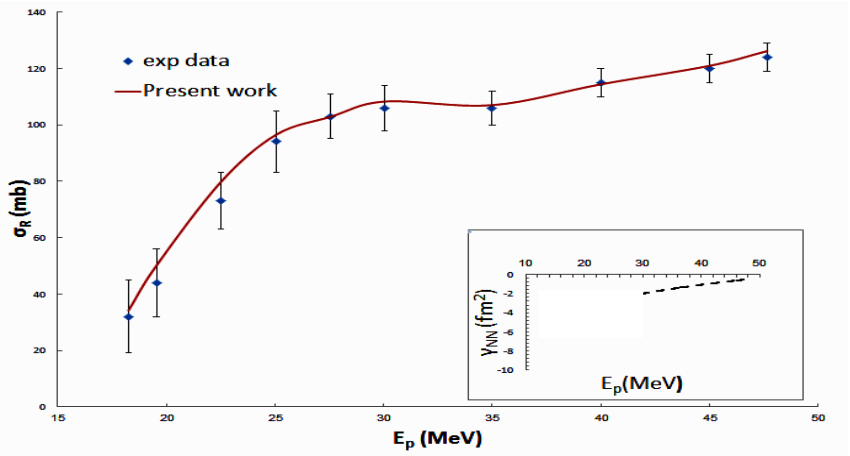

Fig.(3): σ_R for p – ^{3}He using the density of Eq. (9) , σ^t_{NN} is σ^t_{NN} (phenom.) with $\rho = \rho_0 = 0$ fm $^{-3}$ and ε_{NN} , are from Eq.(21), $\gamma_{3BF} = \lambda_n = 0$ and β_{NN} from Eq. (18).

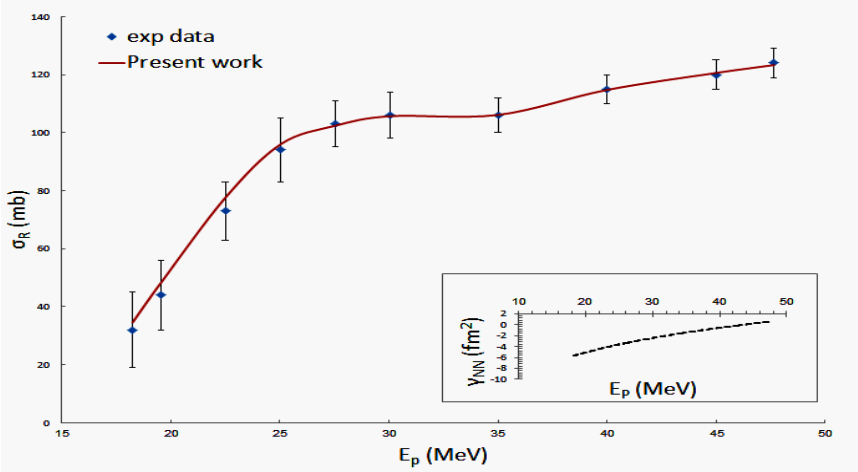

Fig. (4): As Fig.(3) with $\rho = \rho_0 = 0.17$ fm $^{-3}$

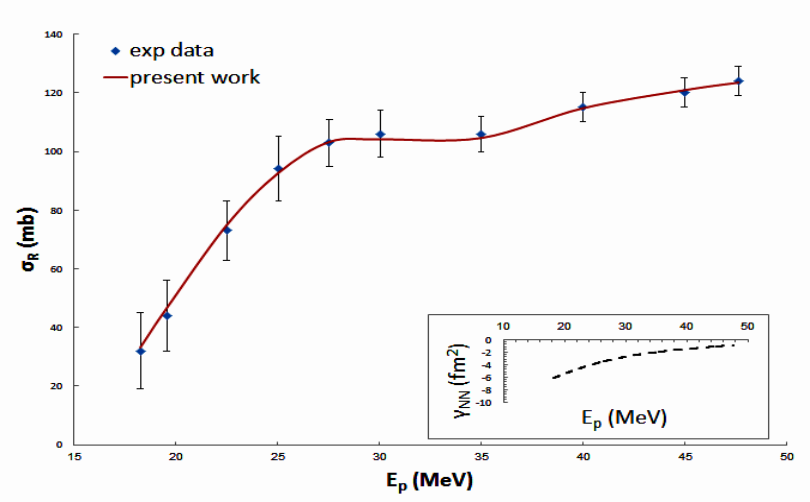

Fig. (5): σ_R for $p - {}^3He$ using the density from Eq. (13). σ^t_{NN} is σ^t_{NN} (phenom) with $\rho = \rho_0 = 0$ fm $^{-3}$ and ε_{NN} from Eq.(21), $\gamma_{3BF} = \lambda_n = 0$ and β_{NN} from Eq. (18).

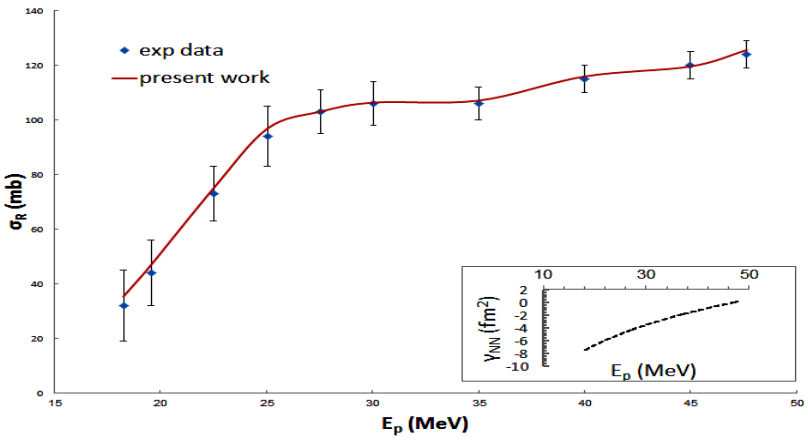

Fig. (6): As Fig.(5) with $\rho = \rho 0 = 0.17$ fm $^{-3}$

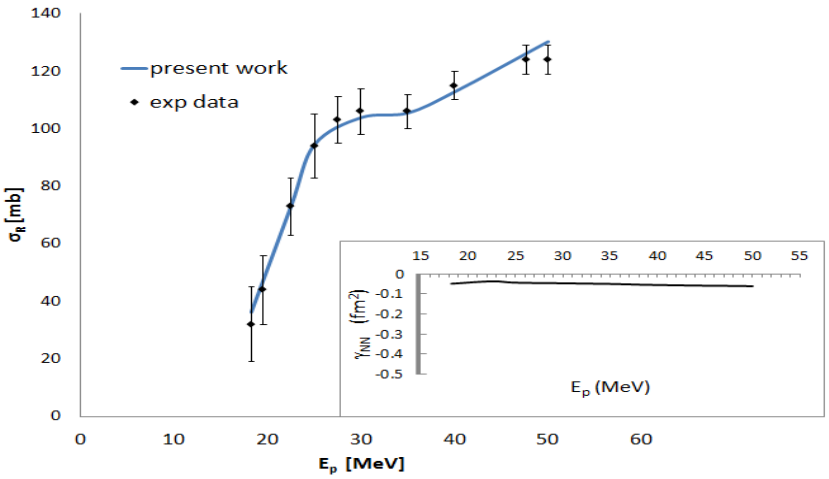

Fig. (7): σ_R for p – ^{3}He using the density distribution from Eq. (9) with $\gamma_{3BF} = 0$. σ^t_{NN} and ε_{NN} are from Eqs.(15) and (19) respectively, while β from Eq. (18), λ_n is represented in Table (2).

Table (2): The values of λ_{nn} (n=1 and 2)which give a best fit for σ_R as described in Figs.(7) and (8).

Energy (MeV)	λ_1 (fm^4)	λ_2 (fm^6)
18.25	0.406 +i 1.360	0.033 - i 0.268
22.50	0.308 + i 0.880	0.026 – i 0.216
25.00	0.260 + i 0.710	0.020 - i 0.170
30.00	0.170 + i 0.430	0.010 - i 0.120
35.00	0.110 + i 0.210	0.009 - i 0.090
40.00	0.060 + i 0.160	0.004 - i 0.060
50.00	0.030 + i 0.100	0.003 - i 0.060

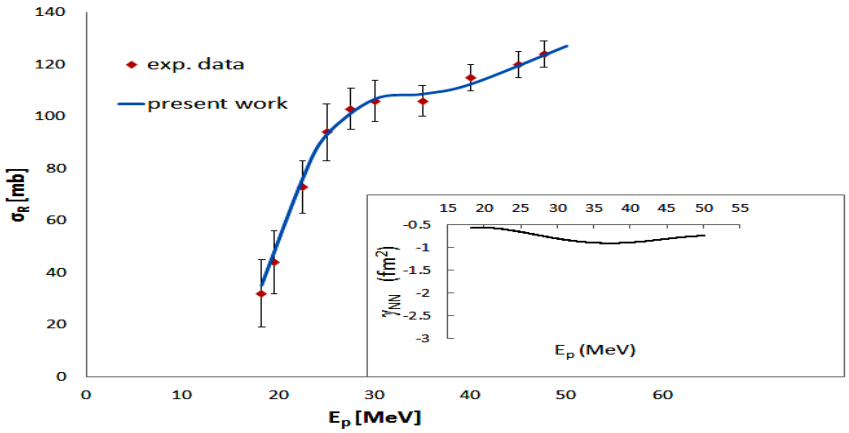

Fig. (8): As Fig. (7) but using the density distribution from Eq. (13)

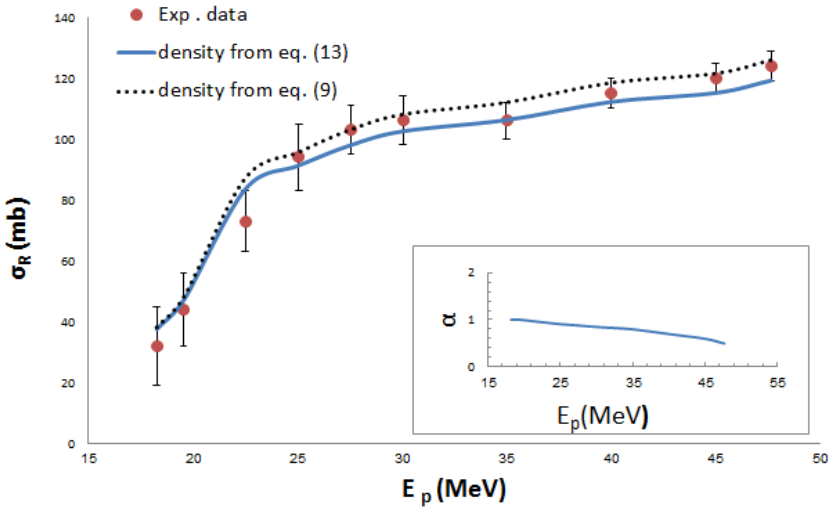

Fig. (9): σ_R for p – ^{3}He using modified NN total cross section according to Pauli blocking as in Eq.(25). $\gamma_{3BF} = \gamma_{NN} = \lambda_n = 0$.

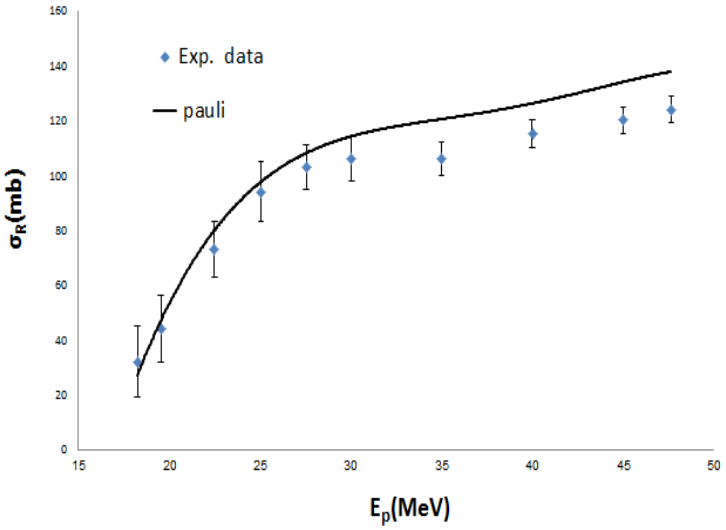

Fig. (10): σ_R for p – ^{3}He using Eq.(26) .

Table (3): σ_R for $\bar{p} - {}^3He$. The experimental data are taken from[41] .$\gamma_{NN} = \lambda_n = 0$.

$E_{\bar{p}}$ (MeV)	σ_R [mb]					
	Using eq. [9]			Using eq. [13]	Using eq. [13],h=0	Exp. data
	$\gamma_{3BF} = 0$	$\gamma_{3BF} = 0.02$	$\gamma_{3BF} = 0.04$			
19.6	382.65	382.65	382.65	401.28	383.94	392 ∓ 23
21.1	375.88	375.88	375.88	394.28	377.13	
46.8	305.52	305.53	305.53	321.80	306.49	
49.2	301.41	301.41	301.42	317.58	302.36	
50	300.08	300.09	300.09	316.21	301.03	
98.6	249.15	249.16	249.17	263.71	249.87	
138.4	227.73	227.74	227.74	241.42	228.32	
141.6	226.37	226.38	226.39	239.99	226.95	
180.9	212.69	212.70	212.71	225.63	213.18	
194	208.97	208.98	208.98	221.69	209.42	
232	200.00	200.01	200.02	212.18	200.37	
238.4	198.67	198.68	198.69	210.77	199.03	
250	196.49	196.50	196.51	208.45	196.83	
294.8	188.97	188.98	188.99	200.40	189.23	
300	188.11	188.12	188.13	199.47	188.36	
305	187.46	187.47	187.49	198.77	187.71	
350	181.60	181.61	181.63	192.46	181.78	
508	167.08	167.10	167.12	176.69	167.10	
521.2	166.08	166.10	166.12	175.60	166.09	
565	163.17	163.19	163.21	172.41	163.14	
757	153.16	153.18	153.20	161.44	153.02	
1014.6	143.83	143.86	143.88	151.18	143.60	
1070	142.21	142.24	142.26	149.40	141.96	

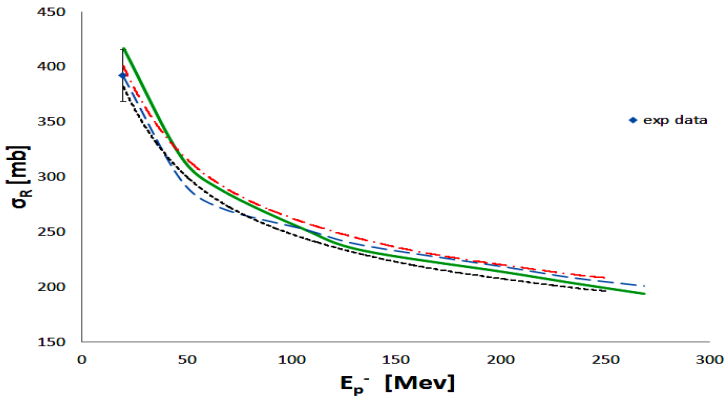

Fig. (11): σ_R for $\bar{p} - {}^3He$. The parameters of $\bar{p}N$ amplitude is taken from Eqs.(22-24), γ_{NN}=0. The density is considered from Eq.(9), with $\gamma_{3BF} = 0$ and Eq. (13). The solid and dashed lines represent the theoretical data from[41] using models A and D.

Table (4): σ_R for $\bar{p} - {}^3He$ with /without γ_{NN} at 19.6 MeV.

$E_{\bar{p}}$ (Mev)	σ_R (mb)						
	density from eq. (9)		density from eq. (13)		density from eq. (13), h=0		exp. Data
	$\gamma_{NN} = 0$ (fm^2)	$\gamma_{NN} = -.3$ (fm^2)	$\gamma_{NN} = 0$ (fm^2)	$\gamma_{NN} = .3$ (fm^2)	$\gamma_{NN} = 0$ (fm^2)	$\gamma_{NN} = -.3$ (fm^2)	
19.6	382.6	392.1	401.2	392.8	383.9	393.3	392 ± 23

REFERENCES

(1) M.A. Ibrahim, M.M. Tag El-Din, Taha and S.S.A. Hassan, Int.J. Mod.Phys.E23 (2014) 1450010(16 pages).

(2)R. Sayed et al., Phys.Rev.C84(2011)037604.

(3) K. Iida, K. Oyamalsu, B. Abu-Ibrahim and A. Kohama, Prog.Theor. Phys.126 (2011)1091.

(4) B. Abu-Ibrahim et al., Phys. Rev,C 77(2008)034607.

(5) M.A. Ibrahim, M.M. Tag El-Din, S.S.A. Hassan and M.F. Hassan, J. Nucl. and Rad.Phys.5 (2010) 35.

(6) M.A. Alvi, Nucl. Phys. A789 (2007) 73.

(7) M.A. Ibrahim, M.M. Tag El-Din, S.S.A. Hassan and El.K. Elmaghraby and M.M. Al-Garni, Arab J. Nucl. Science and Appl.44(2011)168.

(8) R.J. Glauber, Lecture in Theoretical Physics, eds. W.E. Brittin and L.G. Dunham, Vol.1(Wiley, New York, 1959)315.

(9) M.A. Arafah, Ind. J. Science and Tech. 4(2011)603.

(10) H.Rui et al. Chin. Lett. 30 (2013) 122501.

(11) M.A. Alvi, Braz. J. Phys. 44 (2014) 55.

(12) Ed.V. Hungerford, Nucl. Phys. A585 (1995) 121C.

(13) D. Marlaw, et al., Phys. Rev. C25 (1982) 2619.

(14) BNL Experiment 874, E.V. Hungerford (spokesperson); K. Hiks, Proc. of the Conference on the interactions of particle and nuclear physics, June 1994.

(15) E.I. Tanaka and H. Horiuchi, Phys. Rev. C54 (1996) 3170.

(16) C. Xiagzhou et al., Phys. Rev. C58 (1998) 572.

(17) A. One, H. Horiuchi, T. Maruyama and A. Ohnishi, Phys. Rev. Lett. 6 8 (1992) 2898, Prog. Theor. Phys. 87 (1992)1182.

(18) G.Q. li and R. Machleidt, Phys. Rev. C48 (1993) 1702.

(19) B. Chen, F. Sammarruca and C.A. Bertulani, Phys. Rev. C (2013) 054616.

(20) S.K. Charagi and S.K. Gupta, Phys. Rev. C41 (1990) 1610.

(21) D. Chauhan and Z.A. Khan, Phys. Rev. C80 (2009) 054601, Eur. Phys. J. A41 (2009) 179.

(22) V. Franco and G.K. Varma, Phys. Rev. C18 (1978) 349.

(23) Y. Nogami and N. Ohtsuka, Phys. Rev. C23 (1981) 1759.
(24) M.A. Hassan and S.S.A. Hassan, J. Phys. G: Nucl. Part. Phys. 17(1991)1177.
(25) J.S. McCarthy, I. Sick and R.R. Whitney, Phys. Rev. C15 (1977) 1396.
(26) P.J. Mohr, B.N. Taylor and D.M. Newell, Rev. Mod. Phys. 84 (2012) 1527.
(27) M. Kohno, M. Higashi, Y. Watanabe and M. Kawai, Phys. Rev. C57 (1998) 3495.
(28) C.A. Bertulani and C.De. Conti, Phys. Rev. C81 (2010) 064603.
(29) W. Horiuchi, Y. Suzuki, B. Abu-Ibrahim and A. Kohama, Phys. Rev. C75 (2007) 044607.
(30) R.F. Carlson, Atomic Data and Nuclear Data Tables 63 (1996) 93.
(31) R.E. Warner, I.J. Thompson and J.A. Tostevin, Phys. Rev. C65 (2002) 044617.
(32) M.A.M. Hassan et al., Aust. J. Phys. 49 (1996) 655.
(33) M.A.M. Hassan, Acta Phys. Pol. B32 (2001) 2221.
(34) A.S. Shalaby and H. El-Gogary, Prog, Phys.3(2007)5.
(35) A. Rios and V. Soma, Phus. Rev. Lett. 108 (2012) 012501.
(36) O. Lopez et al., Phys. Rev.C90 (2014) 064601.
(37) M.S. Hussein, R.A. Rego and C.A. Bertulani, Phys. Rep. 201 (1991) 279.
(38) H.F. Arellano and M. Girod, Phys. Rev. C76 (2007) 034602.
(39) M.A. Alvi, Int. J. Pure and Appl. Phys. 4 (2008) 65.
(40) M.R. Arafah, Ind. J. Science and Tech.4 (2011) 603.
(41) Yu.N. Uzikov, J. Haidenbauer and B.A. Prwantayeva, Phys. Rev. C84 (2011) 054011.
(42) A.G. Sitenko, Fiz. Elem. Chastits At. Yadra4 (1973) 546 [Sov. J. Part. Nuclei4 (1973) 231].